

## Discovery of a novel fluorescent HSP90 inhibitor and its anti-lung cancer effect†

Su-Yun Bai,<sup>‡ac</sup> Xi Dai,<sup>‡b</sup> Bao-Xiang Zhao<sup>\*b</sup> and Jun-Ying Miao<sup>\*a</sup>

Cite this: *RSC Adv.*, 2014, 4, 19887

Received 1st March 2014  
Accepted 2nd April 2014

DOI: 10.1039/c4ra01800a

www.rsc.org/advances

A series of novel fluorescent pyrazoline coumarin derivatives were synthesized. From them, we screened a compound possessing strong growth inhibitory effects on lung cancer cells. By taking advantage of fluorescence combined with LC-MS/MS and chemoinformatics technique, we successfully identified HSP90 as the target of the compound.

Drug target deconvolution is vital in new drug discovery.<sup>1</sup> It is not only helpful for elucidating the biological mechanism of disease, rational drug design and efficient structure–activity relationship (SAR) studies, but also beneficial for early discovery of side effects and toxicity of drugs.<sup>2</sup> Despite chemical proteomics facilitating drug target identification and verification, drug target deconvolution is still difficult to achieve.<sup>3</sup> Fluorescent drugs, based on synthetic small molecules, are potent tools to monitor biological events in a living system.<sup>4,5</sup> Fluorescence emitted by drugs can also be helpful for drug target identification.<sup>6</sup> However, to date, due to limitations such as cell permeability, *in vivo* activity and toxicity, very few fluorescent anti-cancer drugs have been developed.

Many pyrazoline derivatives are known to display a wide range of biological activities such as anti-inflammatory,<sup>7</sup> anti-malarial,<sup>8</sup> antitumor,<sup>8</sup> antidepressants and anticonvulsant<sup>9</sup> activity. Coumarin is an old compound, which has recently drawn much attention due to its broad pharmacological

activity. Many coumarins and their derivatives show anti-tumor, anti-inflammatory, anti-coagulant and anti-oxidant effects, as well as anti-microbial and enzyme inhibition properties.<sup>10</sup> In addition, pyrazoline and coumarin are also used as fluorescent chromophores.<sup>11–15</sup> Here, we synthesized a series of fluorescent pyrazoline coumarin derivatives and evaluated their anti-lung cancer proliferation activity. By taking advantage of fluorescence combined with LC-MS/MS and chemoinformatics technique, we identified the target of screened compound **3e**.

As a molecular chaperone, heat shock protein 90 (HSP90) is involved in folding and stabilization of some client proteins, which regulate the survival of cancer cells. Thus, HSP90 inhibitors are promising therapeutic agents for cancer treatment. Currently, some HSP90 inhibitors include geldanamycin and its derivatives (*i.e.*, tanespimycin, alvespimycin, IPI-504), synthetic and small molecule inhibitors (*i.e.*, AU922, AT13387, STA9090, MPC3100), and other inhibitors of HSP90 and its isoforms (*i.e.*, shepherdin).<sup>16,17</sup> However, limitations such as cytotoxicity and poor solubility demand the development of novel compounds targeting HSP90. Here, we synthesized a novel fluorescent HSP90 inhibitor, which showed strong growth inhibitory effects on lung cancer cells.

Compounds **3a–3e** were synthesized from substituted chromenone **1** according to reported methods (Scheme 1).<sup>18,19</sup> The structures of the compounds were characterized by <sup>1</sup>H NMR, IR,

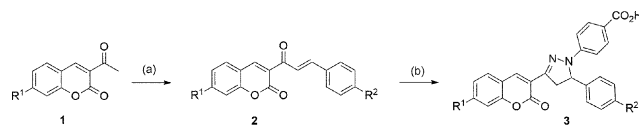
<sup>a</sup>Institute of Developmental Biology, School of Life Science, Shandong University, Jinan 250100, P.R. China. E-mail: miao jy@sdu.edu.cn; Fax: +86 531 88565610; Tel: +86 531 88364929

<sup>b</sup>Institute of Organic Chemistry, School of Chemistry and Chemical Engineering, Shandong University, Jinan 250100, P.R. China. E-mail: bxzhao@sdu.edu.cn

<sup>c</sup>School of Basic Medical Sciences, Taishan Medical University, Taian 271000, P.R. China

† Electronic supplementary information (ESI) available: Details of experimental procedures, data for growth inhibition, LC-MS/MS, chemoinformatics prediction, molecular docking, crystal structure, IR, <sup>1</sup>H NMR and <sup>13</sup>C spectra, HRMS. CCDC 986432. For ESI and crystallographic data in CIF or other electronic format see DOI: 10.1039/c4ra01800a

‡ Equal contribution.



a: R<sup>1</sup> = R<sup>2</sup> = H;  
b: R<sup>1</sup> = H, R<sup>2</sup> = OCH<sub>3</sub>;  
c: R<sup>1</sup> = H, R<sup>2</sup> = 3,4-OCH<sub>2</sub>O;  
d: R<sup>1</sup> = H, R<sup>2</sup> = OH;  
e: R<sup>1</sup> = N, N-2C<sub>2</sub>H<sub>5</sub>, R<sup>2</sup> = H;

(a) substituted benzaldehyde, piperidine, EtOH, reflux 1-30 h; (b) 4-hydrazinylbenzoic acid, acetic acid, EtOH, reflux 4-7 h;

Scheme 1 Synthesis of compound **3a–3e**.

and MS. Moreover, representative crystal structure (**3e**) was determined by X-ray diffraction analysis (Fig. S1, ESI<sup>†</sup>).

The morphology study (Fig. S2, ESI<sup>†</sup>) and viability assay (Fig. S3, ESI<sup>†</sup>) of the A549 lung cancer cells treated with pyrazoline coumarin derivatives **3a–3e** for 48 h were performed. Results showed compounds **3a–3e** could inhibit the growth of A549 cells. Among these pyrazoline coumarin derivatives, compound **3e** had the most powerful anti-proliferation effect ( $IC_{50}$  at 48 h = 7.9  $\mu$ M, see Table. S1, ESI<sup>†</sup>). Further study indicated that compound **3e** also strongly inhibited H322 and H1299 growth of lung cancer cells (Fig. S4 and Table. S1, ESI<sup>†</sup>), but it had no inhibitory effect on the growth of normal cells HUVECs (Fig. S4, ESI<sup>†</sup>). Moreover, the study on the anti-proliferation mechanism of these compounds showed that compound **3e** at 20  $\mu$ M could induce apoptosis (Fig. S5, ESI<sup>†</sup>) rather than autophagy (Fig. S6, ESI<sup>†</sup>) and necrosis (Fig. S7, ESI<sup>†</sup>) in A549 cells, while other compounds, within the test range of concentration, did not cause apoptosis (Fig. S5, ESI<sup>†</sup>), autophagy (Fig. S6, ESI<sup>†</sup>) and necrosis (Fig. S7, ESI<sup>†</sup>) in A549 cells. Therefore, compound **3e** is a promising anti-cancer small molecule.

Fluorescent imaging of compounds **3a–3e** in A549 cells was performed by fluorescence microscopy. After incubation of A549 cells with 20  $\mu$ M of compound **3e** for 2 h, strong fluorescence could be seen in the cytoplasm of A549 cells, which offers a visual evidence of the compound entering into cells and the pattern of the intracellular distribution (Fig. 1a). Moreover, at 36 h after treatment, fluorescence images of the cells revealed obvious morphological changes such as shrinkage or disorder in cell shape (Fig. 1b), implying that the fluorescence distribution of compound **3e** could be useful for monitoring apoptosis processes. Note that other compounds exhibited no obvious fluorescence.

In order to identify the target of compounds, cell lysates from A549 cells treated with compounds **3a–3e** were analyzed by Native PAGE. Results showed that the lane of compound **3e** treatment proteins had a strong fluorescence strip; however,

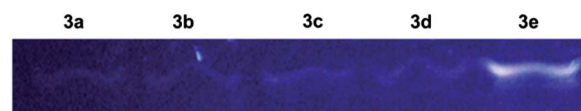


Fig. 2 Native PAGE analysis of total cell lysates from A549 cells treated with 20  $\mu$ M of compounds **3a–3e** for 24 h.

other compounds did not exhibit strong fluorescence signal (Fig. 2). Then, the strong fluorescence strip was cut and analyzed by LC-MS/MS. The results of LC-MS/MS are shown in Table S2.† Small molecules with similar chemical structures often bind to similar targets.<sup>20</sup> Chemical similarities between drugs and ligand sets have helped successfully predict and experimentally test many unanticipated drug targets.<sup>21</sup> PubChem (<http://pubchem.ncbi.nlm.nih.gov>), hosted by the US National Institutes of Health, is a public database for the biological properties of small molecules.<sup>22</sup> Information on drug-target interactions prediction is freely available for academic research on PubChem.<sup>23</sup> Thus, prediction of protein targets was performed using this database and the results are shown in Fig. S8 and S9 (ESI<sup>†</sup>). Then, the overlap of the PubChem prediction results and the LC-MS/MS results revealed that HSP90 was the unique shared protein target.

Previously, we had noted that the binding of a small molecule to its protein target could interfere with the interaction between its protein target and corresponding antibody in cell lysates.<sup>24</sup> Thus, we used the monoclonal antibody of HSP90 against full length recombinant HSP90 to immunoprecipitate HSP90 and examine whether compound **3e** could interfere with this process. The results showed that the compound blocked the binding of HSP90 with its antibody in a dose-dependent way, suggesting that the compound might directly bind to HSP90 (Fig. S10, ESI<sup>†</sup>).

To clarify the probable interaction mode between compound **3e** and HSP90, the compound was docked into the crystal structure of HSP90. Results showed that the compound can be easily accommodated into the socket of HSP90 catalytic site with ATPase activity (Fig. S11, ESI<sup>†</sup>).

The function of HSP90, is an crucial molecular chaperone, is to assist nascent proteins and misfolded proteins adopt correct conformations.<sup>25</sup> When HSP90 is exposed to its inhibitors, the amount of its client proteins will decrease due to degradation by the ubiquitin–proteasome system. Client proteins usually are specific oncogenic proteins in different cancer types.<sup>16</sup> The levels of some HSP90 client proteins in A549 cells treated with compound **3e** were determined by western blot. The results showed after treatment with 20  $\mu$ M of compound **3e** for 24 h, there was a statistically significant decrease in p-AKT, AKT and NF- $\kappa$ B (p65), which is a downstream protein of HSP90 client protein I $\kappa$ B (Fig. 3). Moreover, the inhibition of HSP90 is often accompanied by the rise of HSP90 itself or other heat shock proteins.<sup>26,27</sup> However, like the newly discovered HSP90 inhibitor oleocanthal,<sup>28</sup> compound **3e** did not increase the levels of HSP90 and HSP70, indicating compound **3e** and oleocanthal had a different mechanism of action from common inhibitors (Fig. 3).

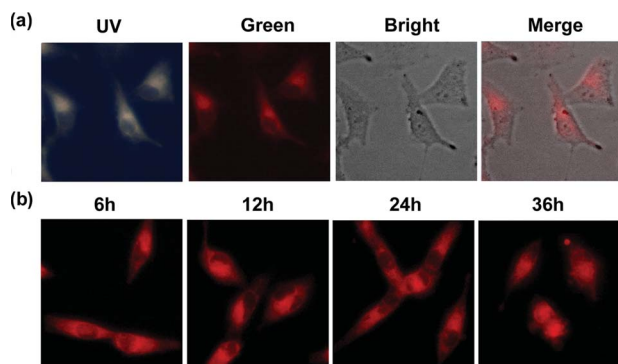


Fig. 1 Fluorescence microscopy images of the intracellular compound **3e** distribution in A549 cells. (a) Cells were incubated with 20  $\mu$ M of compound **3e** for 2 h and photographed under different excitation light and bright light. Overlaid image was also presented. (b) Cells were incubated with 20  $\mu$ M of compound **3e** for 6, 12, 24 and 36 h and photographed under green excitation light.

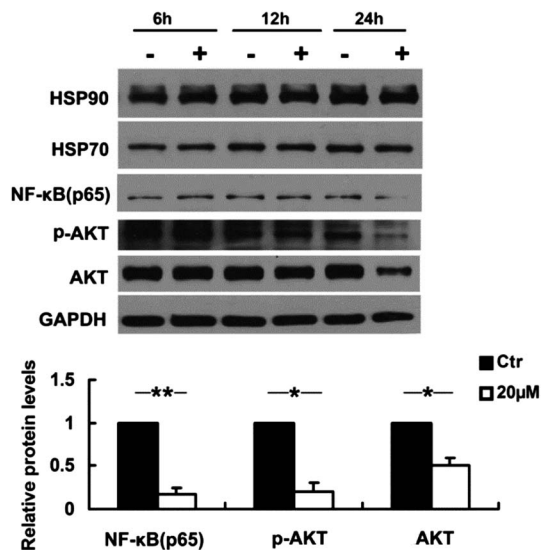


Fig. 3 Western blot analysis of HSP90, HSP70, NF- $\kappa$ B (p65), p-AKT, AKT and GAPDH proteins in A549 cells treated for different times with 20  $\mu$ M of compound **3e**. The graph represented the quantitation of NF- $\kappa$ B (p65), p-AKT and AKT protein levels in A549 cells treated for 24 h with 20  $\mu$ M of compound **3e**. Data are mean  $\pm$  SEM. \* $p$  < 0.05, \*\* $p$  < 0.01,  $n$  = 3. The inset is a representative from three independent experiments.

## Conclusions

Due to its critical role in regulating the stability, activity and intracellular sorting of the client proteins, involved in multiple oncogenic processes, HSP90 is an actively pursued protein target in anti-cancer drug development. However, no HSP90 inhibitor has been FDA-approved to date. Problems such as cytotoxicity and poor solubility demand the development of novel compounds targeting HSP90.<sup>16</sup> Here, we synthesized a novel HSP90 inhibitor with dual function of exhibiting fluorescence and strong growth inhibitory effects on lung cancer cells. Thus far, no fluorescent HSP90 inhibitor has been reported. The fluorescence emitted by drug molecule is very useful for monitoring the drug distribution, concentration and pathways travelled by a drug in cells or even in a living body, which is still a challenge in pharmacokinetic studies.<sup>29</sup> Thus, the new fluorescent HSP90 inhibitor synthesized by us would be of great value in pharmaceutical research and in designing of new therapeutics with improved properties and fewer side effects.

## Acknowledgements

This study was supported by National Natural Science Foundation of China (20972088, 90813022 and 91313303).

## Notes and references

1 G. C. Terstappen, C. Schlupen, R. Raggiacchi and G. Gaviraghi, *Nat. Rev. Drug Discovery*, 2007, **6**, 891–903.

- 2 K. Wang, T. Yang, Q. Wu, X. Zhao, E. C. Nice and C. Huang, *Expert Rev. Proteomics*, 2012, **9**, 293–310.
- 3 B. Lomenick, R. W. Olsen and J. Huang, *ACS Chem. Biol.*, 2011, **6**, 34–46.
- 4 M. J. Uddin, B. C. Crews, A. L. Blobaum, P. J. Kingsley, D. L. Gorden, J. O. McIntyre, L. M. Matrisian, K. Subbaramaiah, A. J. Dannenberg, D. W. Piston and L. J. Marnett, *Cancer Res.*, 2010, **70**, 3618–3627.
- 5 T. Terai and T. Nagano, *Eur. J. Appl. Physiol.*, 2013, **465**, 347–359.
- 6 J. Son, J. J. Lee, J. S. Lee, A. Schuller and Y. T. Chang, *ACS Chem. Biol.*, 2010, **5**, 449–453.
- 7 M. E. Shoman, M. Abdel-Aziz, O. M. Aly, H. H. Farag and M. A. Morsy, *Eur. J. Med. Chem.*, 2009, **44**, 3068–3076.
- 8 B. Insuasty, A. Montoya, D. Becerra, J. Quiroga, R. Abonia, S. Robledo, I. D. Velez, Y. Upegui, M. Nogueras and J. Cobo, *Eur. J. Med. Chem.*, 2013, **67**, 252–262.
- 9 Z. Ozdemir, H. B. Kandilci, B. Gumusel, U. Calis and A. A. Bilgin, *Eur. J. Med. Chem.*, 2007, **42**, 373–379.
- 10 M. E. Riveiro, N. De Kimpe, A. Moglioni, R. Vazquez, F. Monczor, C. Shayo and C. Davio, *Curr. Med. Chem.*, 2010, **17**, 1325–1338.
- 11 S. Q. Wang, Q. H. Wu, H. Y. Wang, X. X. Zheng, S. L. Shen, Y. R. Zhang, J. Y. Miao and B. X. Zhao, *Biosens. Bioelectron.*, 2013, **55C**, 386–390.
- 12 S. Q. Wang, Q. H. Wu, H. Y. Wang, X. X. Zheng, S. L. Shen, Y. R. Zhang, J. Y. Miao and B. X. Zhao, *Analyst*, 2013, **138**, 7169–7174.
- 13 T.-T. Zhang, F.-W. Wang, M.-M. Li, J.-T. Liu, J.-Y. Miao and B.-X. Zhao, *Sens. Actuators, B*, 2013, **186**, 755–760.
- 14 Z. Zhang, F. W. Wang, S. Q. Wang, F. Ge, B. X. Zhao and J. Y. Miao, *Org. Biomol. Chem.*, 2012, **10**, 8640–8644.
- 15 A. Helal, M. H. Or Rashid, C.-H. Choi and H.-S. Kim, *Tetrahedron*, 2011, **67**, 2794–2802.
- 16 D. S. Hong, U. Banerji, B. Tavana, G. C. George, J. Aaron and R. Kurzrock, *Cancer Treat. Rev.*, 2013, **39**, 375–387.
- 17 A. A. Khalil, N. F. Kabapy, S. F. Deraz and C. Smith, *Biochim. Biophys. Acta*, 2011, **1816**, 89–104.
- 18 H. S. Jung, T. Pradhan, J. H. Han, K. J. Heo, J. H. Lee, C. Kang and J. S. Kim, *Biomaterials*, 2012, **33**, 8495–8502.
- 19 S. Khode, V. Maddi, P. Aragade, M. Palkar, P. K. Ronad, S. Mamledesai, A. H. Thippeswamy and D. Satyanarayana, *Eur. J. Med. Chem.*, 2009, **44**, 1682–1688.
- 20 A. Koutsoukas, B. Simms, J. Kirchmair, P. J. Bond, A. V. Whitmore, S. Zimmer, M. P. Young, J. L. Jenkins, M. Glick, R. C. Glen and A. Bender, *J. Proteomics*, 2011, **74**, 2554–2574.
- 21 M. J. Keiser, V. Setola, J. J. Irwin, C. Laggner, A. I. Abbas, S. J. Hufeisen, N. H. Jensen, M. B. Kuijer, R. C. Matos, T. B. Tran, R. Whaley, R. A. Glennon, J. Hert, K. L. Thomas, D. D. Edwards, B. K. Shoichet and B. L. Roth, *Nature*, 2009, **462**, 175–181.
- 22 Y. Wang, J. Xiao, T. O. Suzek, J. Zhang, J. Wang and S. H. Bryant, *Nucleic Acids Res.*, 2009, **37**, W623–W633.
- 23 M. Kuhn, M. Campillos, P. Gonzalez, L. J. Jensen and P. Bork, *FEBS Lett.*, 2008, **582**, 1283–1290.

- 24 H. Li, N. Liu, S. Wang, L. Wang, J. Zhao, L. Su, Y. Zhang, S. Zhang, Z. Xu, B. Zhao and J. Miao, *Biochim. Biophys. Acta*, 2013, **1833**, 2092–2099.
- 25 D. Hanahan and R. A. Weinberg, *Cell*, 2011, **144**, 646–674.
- 26 R. Bao, C. J. Lai, H. Qu, D. Wang, L. Yin, B. Zifcak, R. Atoyian, J. Wang, M. Samson, J. Forrester, S. DellaRocca, G. X. Xu, X. Tao, H. X. Zhai, X. Cai and C. Qian, *Clin. Cancer Res.*, 2009, **15**, 4046–4057.
- 27 T. Khong and A. Spencer, *Mol. Cancer Ther.*, 2011, **10**, 1909–1917.
- 28 L. Margarucci, M. C. Monti, C. Cassiano, M. Mozzicafreddo, M. Angeletti, R. Riccio, A. Tosco and A. Casapullo, *Chem. Commun.*, 2013, **49**, 5844–5846.
- 29 D. Kim, H. Lee, H. Jun, S. S. Hong and S. Hong, *Bioorg. Med. Chem.*, 2011, **19**, 2508–2516.